Acta Cryst. (1990). B**46**, 731–735

High-Temperature (350 K) Orthorhombic Framework Structure of Zeolite H-ZSM-5

By H. van Koningsveld

Laboratories of Applied Physics and Organic Chemistry, Delft University of Technology, Lorentzweg 1, 2628 *CJ Delft, The Netherlands*

(*Received* 21 *May* 1990; *accepted* 27 *June* 1990)

Abstract

$Si_{11\cdot96}Al_{0\cdot04}O_{24}$ ($+0\cdot04H^+$), $M_r = 720\cdot96$, orthorhombic, *Pnma*, $a = 20\cdot078$ (6), $b = 19\cdot894$ (7), $c = 13\cdot372$ (3) Å, $V = 5431$ (9) Å^3, $Z = 8$, $D_x = 1\cdot80$ g cm^{-3}, λ(Mo $K\alpha$) = 0·71069 Å, $\mu = 6\cdot64$ cm^{-1}, $F(000) = 2879\cdot7$, $T = 350$ K, $R = 0\cdot040$ for 3957 observed reflections with $I > 2\cdot0\sigma(I)$. The high-temperature 'empty' orthorhombic framework of (calcined) H-ZSM-5 is not essentially different from the room-temperature orthorhombic framework of as-synthesized ZSM-5, containing the tetrapropylammonium cation as a template. The organic template hardly influences the orthorhombic framework geometry: the maximum observed differences between corresponding Si—O distances, and OSiO and SiOSi angles in both orthorhombic frameworks are 0·017 (4) Å, 1·4 (3) and 3·9 (4)°, respectively; in both frameworks the maximum pore size in the straight channels is ~5·7 Å and the diameter of the nearly circular effective cross-sectional area in the sinusoidal channels is ~5·3 Å. Therefore, two recent reports on H-ZSM-5, describing the atomic scale mechanism of the orthorhombic/monoclinic phase transition [van Koningsveld, Jansen & van Bekkum (1990). *Zeolites*, **10**, 235–242] and a possible diffusion pathway of *p*-xylene [van Koningsveld, Tuinstra, van Bekkum & Jansen (1989). *Acta Cryst.* **B45**, 423–431] by comparing the orthorhombic framework of as-synthesized ZSM-5 with the monoclinic framework of H-ZSM-5, are essentially correct.

Introduction

The ideal framework of as-synthesized ZSM-5, with orthorhombic *Pnma* symmetry, can be constructed in the following way. The (010) pentasil layer with double 10-rings of the straight channels (Fig. 1*a*) is generated by applying successively a twofold screw operation and an inversion to a building unit containing 12 *T* sites (*T* = Si, Al). The three-dimensional framework is completed by linking neighbouring (010) layers by reflection through T_4 and T_6 rings. Thereby, a second type of pentasil layer is generated. One of these (100) pentasil layers, containing double 10-rings of the sinusoidal channels, is shown in Fig. 1(*b*).

H-ZSM-5, obtained by calcination of as-synthesized ZSM-5 followed by NH_4^+ exchange and

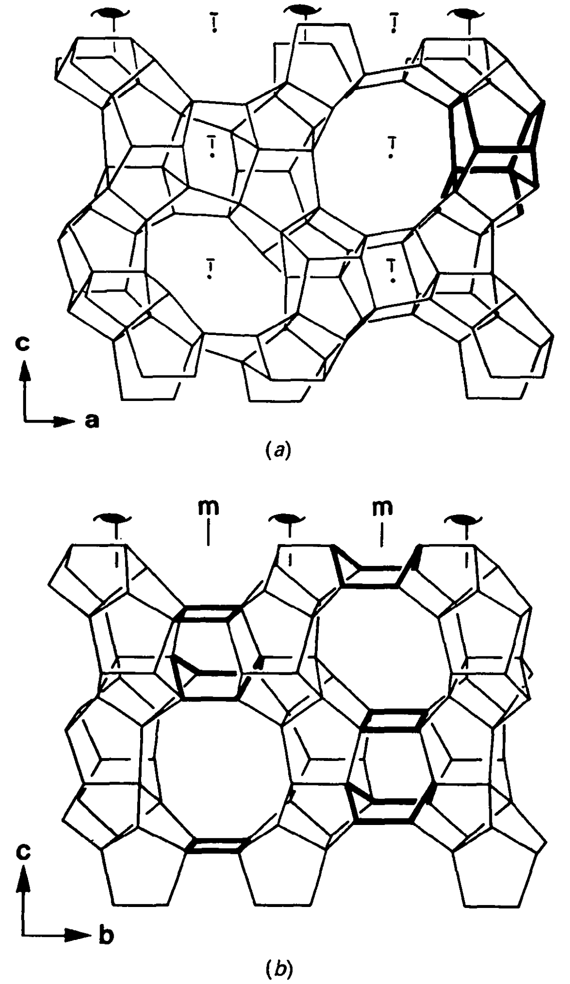

(*a*)

(*b*)

Fig. 1. (010) pentasil layer (*a*) and (100) pentasil layer (*b*) in an orthorhombic ZSM-5 framework. *T* atoms lie at the intersection of lines. O atoms (not drawn) are about midway between the *T* atoms. A T_{12} building unit, T_4 and T_6 rings are indicated by bold lines.

0108-7681/90/060731-05$03.00

a second calcination, shows a reversible structural phase transition at about 340 K (the precise temperature being dependent on the Al content) with no apparent hysteresis. The structure exhibits monoclinic symmetry below and orthorhombic symmetry above the transition temperature (Wu, Lawton, Olson, Rohrman & Kokotailo, 1979; Hay & Jaeger, 1984; Hay, Jaeger & West, 1985; Fyfe, Kennedy, de Schutter & Kokotailo, 1984; Klinowski, Carpenter & Gladden, 1987). Upon cooling, the high-temperature orthorhombic H-ZSM-5 phase (hereafter called HT-ORTHO) changes into an aggregate of twin domains with monoclinic $P2_1/n.1.1$ symmetry (van Koningsveld, Jansen & van Bekkum, 1987). Monoclinic H-ZSM-5 appears to be ferroelastic: application of an appropriate mechanical stress changes the population of the twin domains (van Koningsveld, Tuinstra, Jansen & van Bekkum, 1989). An X-ray analysis of a (nearly) single crystal of monoclinic H-ZSM-5 (hereafter called MONO; van Koningsveld, Jansen & van Bekkum, 1990) revealed that the orthorhombic/monoclinic phase transition, ascribed to a mutual shift of successive (010) layers along $+\mathbf{c}$ or $-\mathbf{c}$, is realized by a complicated displacement of the framework atoms.

In the last report cited it is assumed, as in a recent paper discussing the structure of a *p*-xylene/H-ZSM-5 complex (van Koningsveld, Tuinstra, van Bekkum & Jansen, 1989) that the framework of HT-ORTHO is identical to the framework of orthorhombic as-synthesized ZSM-5 containing the tetrapropylammonium template (hereafter called TPA-ORTHO; van Koningsveld, van Bekkum & Jansen, 1987). This may not be strictly true because of the possible influence of the organic cation on the framework geometry. The present paper reports the framework symmetry and geometry of HT-ORTHO. A comparison with the TPA-ORTHO and MONO frameworks is made.

Experimental

ZSM-5 crystals were obtained as described by Lermer, Draeger, Steffen & Unger (1985) and subsequently converted into H-ZSM-5 (van Koningsveld, Jansen & van Bekkum, 1987). A freshly prepared H-ZSM-5 crystal (with $\mathrm{Si/Al} \simeq 300$), having approximate dimensions of 250 × 175 × 275 μm in **a**, **b** and **c** directions, respectively, was put on a universal high-temperature device for single-crystal diffraction (Tuinstra & Fraase Storm, 1978). The cell dimensions of HT-ORTHO were obtained at 350 ± 4 K by least-squares fitting of the CAD-4 setting angles of 25 reflections with $10 < \theta < 17°$ using graphite-monochromated Mo $K\alpha$ radiation. The systematic extinctions were consistent with space group *Pnma* or $Pn2_1a$. Space group *Pnma* was confirmed by successful refinement. Intensities were measured to $\theta_{\max} = 30{\cdot}0°$ with an $\omega/2\theta$ scan, scan width = $(0{\cdot}95 + 0{\cdot}35\tan\theta)°$ up to $h_{\max} = 28$, $k_{\max} = 27$ and $l_{\max} = 18$. The intensities were measured with 2% accuracy or for a maximum counting time of 120 s. Three reference reflections were measured every 2 h of X-ray measuring time; no systematic change in intensity was observed. Lorentz and polarization corrections were applied but none for extinction or absorption. A unique data set of 7950 reflections, of which 3964 had $I > 2{\cdot}0\sigma(I)$, was obtained. The initial positions of the framework atoms for HT-ORTHO were taken from TPA-ORTHO (van Koningsveld, van Bekkum & Jansen, 1987). All *T* atoms (Si, Al) were treated as Si. The structure was refined in *Pnma* by (blocked) full-matrix anisotropic least-squares refinement to a final $R = 0{\cdot}040$, $wR = 0{\cdot}042$ ($w = 1$) and $S = 0{\cdot}52$ for 332 variables and 3957 observations [3964 with $I > 2{\cdot}0\sigma(I)$ minus seven with $|F_{\text{obs}} - F_{\text{calc}}| > 25{\cdot}0$]. The average and maximum shift/e.s.d. were 0·19 and 0·9 [U_{11} of O(9)], respectively. The final difference Fourier synthesis had $\rho < 0{\cdot}54$ e Å^{-3} with peaks in the close vicinity of the framework atoms. All calculations were performed on the Delft University Amdahl 470/V7B computer using programs of the *XRAY72* system (Stewart, Kruger, Ammon, Dickinson & Hall, 1972). Atomic scattering factors of zero-valent Si and O from Cromer & Mann (1968) were used.

Discussion

Final positional and isotropic thermal parameters in HT-ORTHO are given in Table 1.* Fig. 2 shows the Si-atom numbering used. Distances and angles are summarized in Table 2, together with the corresponding values in TPA-ORTHO (van Koningsveld, van Bekkum & Jansen, 1987) and MONO (van Koningsveld *et al.*, 1990). Table 2 illustrates that, except for the minimum value of the OSiO angle, the ranges of (average) bond lengths and bond angles are essentially the same in both orthorhombic frameworks. The maximum observed difference between corresponding Si—O distances and OSiO angles* in HT- and TPA-ORTHO is 0·017 Å and 1·4°, respectively. These differences are about equal to 4σ(Si—O) and 6σ(OSiO). In MONO, the minimum value of the Si—O distance and the limiting values of the SiOSi angle are clearly different from the corresponding values in the orthorhombic

---

* Lists of structure factors, anisotropic thermal parameters, bond lengths and bond angles have been deposited with the British Library Document Supply Centre as Supplementary Publication No. SUP 53411 (41 pp.). Copies may be obtained through the Technical Editor, International Union of Crystallography, 5 Abbey Square, Chester CH1 2HU, England.

Table 1. *Fractional coordinates* ($\times 10^4$) *and* U_{eq} *values* ($Å^2 \times 10^3$) *of the framework atoms in HT-ORTHO*

$$U_{eq} = \tfrac{1}{3}(U_{11} + U_{22} + U_{33}).$$

	x	y	z	U_{eq}
Si(1)	4229·2 (5)	567·8 (7)	−3350·8 (9)	15·0 (3)
Si(2)	3084·0 (7)	289·7 (6)	−1870·7 (9)	17·1 (3)
Si(3)	2791·9 (6)	619·1 (7)	325·7 (9)	16·9 (3)
Si(4)	1222·8 (6)	639·7 (6)	283·4 (9)	15·1 (3)
Si(5)	716·8 (6)	282·5 (6)	−1841·6 (9)	13·8 (3)
Si(6)	1870·3 (6)	590·6 (7)	−3260·2 (9)	16·8 (3)
Si(7)	4234·6 (6)	−1721·3 (6)	−3233·6 (9)	14·1 (3)
Si(8)	3086·1 (6)	−1292·0 (6)	−1820·6 (9)	16·3 (3)
Si(9)	2741·7 (6)	−1726·9 (6)	334·1 (9)	14·4 (3)
Si(10)	1196·3 (6)	−1732·5 (6)	299·2 (9)	15·1 (3)
Si(11)	704·5 (6)	−1298·1 (6)	−1820·5 (9)	15·0 (3)
Si(12)	1880·3 (6)	−1728·5 (6)	−3167·4 (9)	16·6 (3)
O(1)	3725 (2)	555 (3)	−2437 (3)	44 (1)
O(2)	3093 (2)	594 (2)	−776 (2)	37 (1)
O(3)	2007 (2)	595 (3)	284 (3)	54 (2)
O(4)	953 (2)	633 (2)	−831 (3)	40 (1)
O(5)	1160 (2)	541 (2)	−2747 (3)	33 (1)
O(6)	2433 (2)	533 (3)	−2435 (3)	48 (2)
O(7)	3741 (2)	−1566 (2)	−2335 (3)	42 (1)
O(8)	3085 (2)	−1559 (2)	−699 (3)	42 (1)
O(9)	1969 (2)	−1545 (2)	271 (3)	37 (1)
O(10)	887 (2)	−1629 (2)	−781 (3)	46 (2)
O(11)	1176 (2)	−1576 (2)	2672 (3)	41 (1)
O(12)	2448 (2)	−1556 (3)	−2388 (4)	51 (2)
O(13)	3087 (3)	−499 (2)	−1822 (4)	66 (2)
O(14)	786 (2)	−510 (2)	−1728 (3)	43 (1)
O(15)	4175 (2)	1269 (2)	−3908 (3)	38 (1)
O(16)	4079 (2)	−21 (2)	−4120 (3)	43 (1)
O(17)	4006 (2)	−1329 (2)	−4221 (3)	35 (1)
O(18)	1913 (2)	1302 (2)	−3801 (3)	35 (1)
O(19)	1944 (3)	4 (2)	−4062 (3)	46 (1)
O(20)	1965 (2)	−1297 (2)	−4158 (3)	42 (1)
O(21)	−35 (2)	490 (2)	−2077 (3)	30 (1)
O(22)	−45 (2)	−1490 (2)	−2104 (3)	31 (1)
O(23)	4227 (3)	−2500	−3491 (4)	37 (2)
O(24)	1924 (3)	−2500	−3480 (4)	34 (2)
O(25)	2841 (3)	−2500	596 (4)	28 (2)
O(26)	1100 (3)	−2500	620 (4)	28 (2)

frameworks (see also Fig. 3). Table 3 recapitulates corresponding SiOSi angles and their differences in HT- and TPA-ORTHO. In addition, Table 3 gives the changes in the SiOSi angles caused by the orthorhombic/monoclinic phase transition. From the table it is seen that the differences between corresponding SiOSi angles in HT- and TPA-ORTHO are small, the maximum difference being 3·9° [~ 10σ(SiOSi)]. Therefore, the influence of the organic cation on the orthorhombic framework geometry seems to be of minor importance. In contrast, the differences in SiOSi angles caused by the symmetry change are in general large, especially for large SiOSi angles. Table 3 implicitly shows that the atomic displacements involved in the phase transition of HT-ORTHO to MONO (by cooling down HT-ORTHO) and those involved in the transformation of TPA-ORTHO to MONO (by calcination of TPA-ORTHO) are very similar.

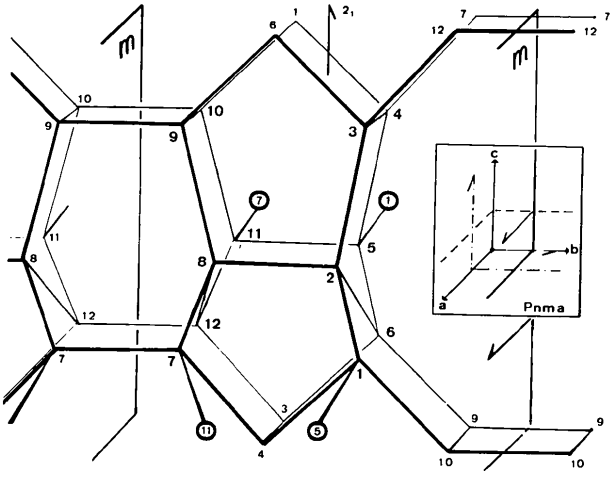

Fig. 2. Part of the (100) pentasil layer showing the *T*-atom numbering used.

Table 2. *Comparison of the framework geometry in HT-ORTHO, TPA-ORTHO and MONO*

	HT-ORTHO	TPA-ORTHO	MONO
O—Si—O range (°)	107·1–111·5 (2)	106·0–112·0 (2)	107·1–111·5 (2)
Average O—Si—O angle/SiO$_4$ (°)	109·5	109·5	109·5
Si—O range (Å)	1·570–1·601 (4)	1·567–1·605 (4)	1·582–1·607 (3)
Range of average Si—O/SiO$_4$ (Å)	1·581–1·593	1·584–1·591	1·588–1·601
Si—O—Si range (°)	145·7–177·7 (4)	144·9–175·9 (4)	141·3–169·0 (3)
Range of average Si(OSi)$_4$ (°)	150·7–163·6	150·5–162·8	147·1–158·8

Table 3. Si(*k*)OSi(*l*) *angles* (°) *in HT-ORTHO, TPA-ORTHO and MONO*

E.s.d.'s ≃0·4° in both ORTHO frameworks and ≃0·3° in MONO.

k,*l*	HT-ORTHO	TPA-ORTHO	$\Delta_{(1)}$[b]	MONO[a]	$\Delta_{(2)}$[c]
3,4	174·7	175·8	−1·1	158·2, 157·2	16·5, 17·5
2,8	177·7	175·9	1·8	159·0, 163·6	18·7, 14·1
8,12	166·7	164·6	2·1	167·1, 153·0	−0·4, 13·7
1,4	166·0	164·8	1·2	169·0, 156·1	−3·0, 9·9
5,11	165·2	169·1	−3·9	157·3, 160·0	7·9, 5·2
3,6	163·2	162·9	0·3	168·5, 153·5	−5·3, 9·7
10,11	161·0	164·4	−3·4	154·5, 158·4	6·5, 2·6
2,6	160·4	158·2	2·2	162·8, 156·6	−2·4, 3·8
7,8	156·3	156·2	0·1	158·2, 149·3	−1·9, 7·0
7,7	155·0	153·3	1·7	156·2	−1·2
4,5	154·6	156·1	−1·5	146·9, 155·5	7·7, −0·9
11,12	154·1	153·5	0·6	156·1, 153·8	−2·0, 0·3
8,9	153·6	154·4	−0·8	151·0, 146·0	2·6, 7·6
1,2	153·1	153·1	0·0	145·0, 153·2	8·1, −0·1
9,10	152·9	154·6	1·7	150·6, 150·1	2·3, 2·8
9,9	150·6	148·0	2·6	151·0	−0·4
2,3	149·6	149·8	−0·2	145·0, 148·9	4·6, 0·7
7,11	149·6	150·4	−0·8	151·1, 147·8	−1·5, 1·8
1,10	148·9	148·2	0·7	150·2, 151·0	−1·3, −2·1
12,12	148·9	146·3	2·6	149·8	−0·9
5,6	148·6	147·9	0·7	149·0, 147·7	−0·4, 0·9
3,12	148·5	147·7	0·8	142·6, 155·3	5·9, −6·8
4,7	147·8	149·4	−1·6	146·0, 149·7	1·8, −1·9
1,5	146·3	145·4	0·9	144·8, 149·7	1·5, −3·4
10,10	145·8	144·9	0·9	145·3	0·5
6,9	145·7	145·1	0·6	141·3, 150·6	4·4, −4·9

Notes: (*a*) In MONO, *m* is lost resulting in two different SiOSi angles except in those cases where Si(*k*) and Si(*l*) were related by *m*. (*b*) $\Delta_{(1)}$ = difference between corresponding SiOSi angles in HT-ORTHO and TPA-ORTHO. (*c*) $\Delta_{(2)}$ = difference between corresponding SiOSi angles in HT-ORTHO and MONO.

Fig. 3 gives the scatter diagram of ⟨*d*(Si—O)⟩, the average *d*(Si—O) in an Si—O—Si bridge, as a function of the SiOSi angle. The figure illustrates that smaller ⟨*d*(Si—O)⟩ involve wider SiOSi angles. In other words: in the region of large SiOSi angles the framework is more contracted. In HT- and TPA-ORTHO, SiOSi angles between 170 and 180° are actually observed, while the maximum observed SiOSi angle in MONO is 169°. The HT- and TPA-ORTHO frameworks seem therefore the more stressed ones. The difference in slope of the regression lines in HT- and TPA-ORTHO is not very pronounced: the template containing the TPA-ORTHO framework seems hardly more stressed than the 'empty' HT-ORTHO framework. This again illustrates the barely noticeable influence of the organic cation on the orthorhombic framework geometry.

Subtle differences in the local framework geometry can be studied by ^{29}Si MAS NMR. The NMR spectra of silica polymorphs and silicates have been interpreted (Smith & Blackwell, 1983; Engelhardt & Radeglia, 1984) on the basis of a quantitative relationship between the average $Si(OSi)_4$ angle and the chemical shift for the $Si(OSi)_4$ signal. A change of ~1° in the average $Si(OSi)_4$ angle corresponds to a chemical shift difference of about 0·6 p.p.m. Since, for highly crystalline materials, NMR peaks separated by 0·1 p.p.m. can be clearly resolved, changes in the mean bond angles of about 0·2° may be detected from the ^{29}Si NMR spectra (Engelhardt & van Koningsveld, 1990*a*). In Table 4 the average $Si(OSi)_4$ angles in HT-ORTHO, TPA-ORTHO and MONO are listed. This table shows that the ^{29}Si MAS NMR spectra of HT- and TPA-ORTHO are expected to be, in principle, distinguishable and that the difference between these spectra and the spectrum of MONO must be considerable. Table 5 summarizes the calculated ^{29}Si chemical shifts in HT- and TPA-ORTHO and in MONO. An extensive discussion on the calculated and observed ^{29}Si NMR spectra of TPA-ORTHO and MONO will appear soon (Engelhardt & van Koningsveld, 1990*a*; Fyfe, 1990). There is good agreement between observed and calculated spectra of MONO. The calculated spectrum of TPA-ORTHO is very similar to the spectra of several sorbate-loaded ZSM-5 frameworks with orthorhombic symmetry. A detailed comparison of the calculated spectrum of HT-ORTHO with observed spectra, recorded in the literature, will be published elsewhere (Engelhardt & van Koningsveld, 1990*b*).

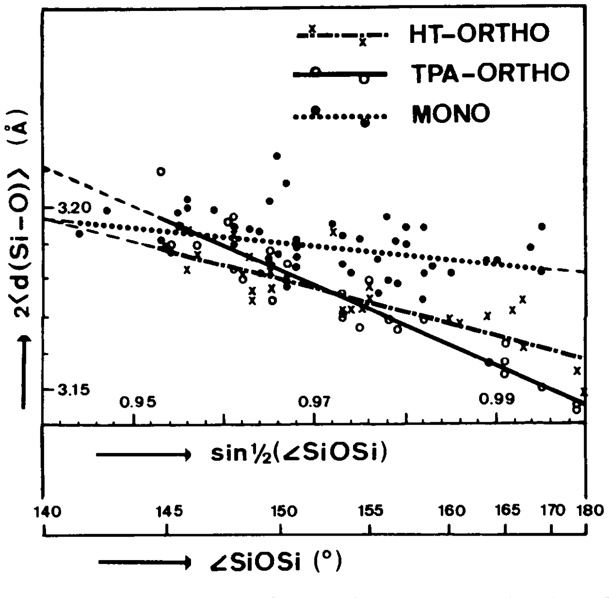

Fig. 3. Scatter diagram of ⟨*d*(Si—O)⟩, plotted as a function of sin½(∠SiOSi) in HT- and TPA-ORTHO and in MONO.

Table 4. *Average* $Si(OSi)_4$ *angles* (°) *in HT-ORTHO, TPA-ORTHO and MONO*

	HT-ORTHO	TPA-ORTHO	$\Delta_{(1)}$[b]	MONO[a]		$\Delta_{(2)}$[c]	
Si(1)	153·6	152·9	0·7	153·5,	151·3	0·1,	2·3
Si(2)	160·2	159·3	0·9	153·0,	155·6	7·2,	4·6
Si(3)	159·0	159·1	−0·1	153·0,	154·3	6·0,	4·7
Si(4)	160·8	161·5	−0·7	152·7,	156·9	8·1,	3·9
Si(5)	153·7	154·6	−0·9	149·5,	153·2	4·2,	0·5
Si(6)	154·5	153·5	1·0	155·4,	152·1	−0·9,	2·4
Si(7)	152·2	152·3	−0·1	152·1,	151·6	0·1,	0·6
Si(8)	163·6	162·8	0·8	158·8,	153·0	4·8,	10·6
Si(9)	150·7	150·5	0·2	150·8,	147·1	−0·1,	3·6
Si(10)	152·2	153·0	−0·8	150·4,	151·0	1·8,	1·2
Si(11)	157·5	159·4	−1·9	154·8,	155·0	2·7,	2·5
Si(12)	154·6	153·0	1·6	153·9,	153·0	0·7,	1·6

Notes: (*a*) Second column gives average angles at Si(13)···Si(24); in HT- and TPA-ORTHO these Si atoms are related to Si(1)···Si(12) by *m*. (*b*) $\Delta_{(1)}$ is the difference between angles in HT-ORTHO and TPA-ORTHO. (*c*) $\Delta_{(2)}$ is the difference between angles in HT-ORTHO and MONO.

Table 5. ^{29}Si *chemical shifts* (δ) *in HT-ORTHO, TPA-ORTHO and MONO*

Calculated from the average $Si(OSi)_4$ values (α) given in Table 4 using the equation (Engelhardt & van Koningsveld, 1990*a*): $\delta = -247{\cdot}05[\cos\alpha/(\cos\alpha - 1)] + 2{\cdot}50$ p.p.m.

Si atom	HT-ORTHO	TPA-ORTHO	MONO*	
9	−112·6	−112·5	−112·6,	−110·2
7	−113·5	−113·5	−113·4,	−113·1
1	−114·2	−113·9	−114·2,	−112·9
10	−113·5	−113·9	−112·4,	−112·8
12	−114·8	−113·9	−114·4,	−113·9
6	−114·7	−114·2	−115·2,	−113·4
5	−114·3	−114·8	−111·8,	−114·0
3	−116·8	−116·8	−113·9,	−114·6
2	−117·3	−116·9	−113·9,	−115·3
11	−116·1	−116·9	−114·8,	−114·9
4	−117·5	−117·7	−113·7,	−115·9
8	−118·5	−118·2	−116·7,	−113·9

* Mono has 24 independent *T* sites. The second number gives the chemical shift of Si(*n* + 12); *e.g.* −110·2 p.p.m. is the chemical shift for Si(9 + 12), *etc.*

Table 6. *Pore openings* (O···O *distances*, Å; *e.s.d.'s* ≃0·006 Å) *in* 10-*rings*

Minimal and maximal O···O distances are underlined. Minimum and maximum pore sizes are calculated using 1·35 Å for the O-atom radius. The O-atom numbering is for use in this table only and is defined as given in the diagram below.

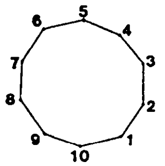

10-rings in the straight channel

	1→6	2→7	3→8	4→9	5→10	Min.	Max.
HT-ORTHO*	7·985	8·250	8·153	8·406	8·033	5·29	5·71
TPA-ORTHO*	7·922	8·124	8·164	8·449	8·081	5·22	5·75
MONO	8·115	7·875	8·484	8·243	8·086	5·18	5·78
	7·969	8·163	8·532	8·487	7·980	5·27	5·83

10-rings in the sinusoidal channel

	1→6	2→7	3→8	4→9	5→10	Min.	Max.
HT-ORTHO	8·308	8·077	8·077	8·308	8·061	5·36	5·61
	7·945	8·042	8·042	7·945	8·382	5·25	5·68
TPA-ORTHO	8·250	8·132	8·132	8·250	7·992	5·29	5·55
	7·983	8·079	8·079	7·983	8·295	5·28	5·60
MONO†	8·593	8·171	8·054	8·113	8·148	5·35	5·89
	8·162	7·712	8·476	7·760	8·400	5·01	5·78

* Second ring related to first one by *m*.

† The mirror plane, present in HT- and TPA-ORTHO through O(5) and O(10), is lost.

Finally, Table 6 compares the pore sizes in those 10-rings in HT-ORTHO, TPA-ORTHO and MONO which mainly govern the sieve and diffusion properties (van Koningsveld *et al.*, 1990). The table shows that the elliptical 10-rings in the straight channel have limiting pores of 5·3 × 5·7 and 5·3 × 5·8 Å in HT-ORTHO and TPA-ORTHO, respectively. The cross-sections in the two independent 10-rings of the sinusoidal channel are 5·4 × 5·6 and 5·3 × 5·7 Å in HT-ORTHO and 5·3 × 5·6 Å (for both 10-rings) in TPA-ORTHO. The small differences between the pore dimensions in both orthorhombic frameworks once more demonstrate that the TPA ion hardly influences the orthorhombic framework geometry. The symmetry change between HT-ORTHO and MONO scarcely affects the pore size in the straight channel. The free area in each 10-ring in the sinusoidal channel, however, changes from nearly circular (diameter ≃5·3 Å) to a more elliptical form.

In conclusion, one can say that, although there are subtle differences which are expected to show up in the ^{29}Si MAS NMR spectra, the framework geometries of HT- and TPA-ORTHO are essentially the same.

In some recent papers (*e.g.* van Koningsveld, Tuinstra, van Bekkum & Jansen, 1989; van Koningsveld *et al.*, 1990) the atomic scale mechanism of the orthorhombic/monoclinic phase transition and a possible diffusion pathway of *p*-xylene in H-ZSM-5 are described by comparing the geometries of the TPA-ORTHO and MONO frameworks. The present structure analysis shows that these descriptions are essentially correct: the influence of TPA on the framework geometry is very small leading to very similar framework geometries for TPA-ORTHO and HT-ORTHO.

The author gratefully thanks J. C. Jansen, Laboratory of Organic Chemistry, Delft University of Technology, for supplying the H-ZSM-5 crystal.

References

Cromer, D. T. & Mann, J. B. (1968). *Acta Cryst.* **A24**, 321–324.

Engelhardt, G. & Radeglia, R. (1984). *Chem. Phys. Lett.* **108**, 271–274.

Engelhardt, G. & van Koningsveld, H. (1990*a*). *Zeolites*, **10**, 650–656.

Engelhardt, G. & van Koningsveld, H. (1990*b*). In preparation.

Fyfe, C. A. (1990). In preparation.

Fyfe, C. A., Kennedy, G. J., de Schutter, C. T. & Kokotailo, G. T. (1984). *J. Chem. Soc. Chem. Commun.* pp. 541–542.

Hay, D. G. & Jaeger, H. (1984). *J. Chem. Soc. Chem. Commun.* p. 1433.

Hay, D. G., Jaeger, H. & West, G. W. (1985). *J. Phys. Chem.* **89**, 1070–1072.

Klinowski, J., Carpenter, T. A. & Gladden, L. F. (1987). *Zeolites*, **7**, 73–78.

Koningsveld, H. van, Jansen, J. C. & van Bekkum, H. (1987). *Zeolites*, **7**, 564–568.

Koningsveld, H. van, Jansen, J. C. & van Bekkum, H. (1990). *Zeolites*, **10**, 235–242.

Koningsveld, H. van, Tuinstra, F., Jansen, J. C. & van Bekkum, H. (1989). *Zeolites*, **9**, 253–256.

Koningsveld, H. van, Tuinstra, F., van Bekkum, H. & Jansen, J. C. (1989). *Acta Cryst.* **B45**, 423–431.

Koningsveld, H. van, van Bekkum, H. & Jansen, J. C. (1987). *Acta Cryst.* **B43**, 127–132.

Lermer, H., Draeger, M., Steffen, J. & Unger, K. K. (1985). *Zeolites*, **5**, 131–134.

Smith, J. V. & Blackwell, C. S. (1983). *Nature* (*London*), **303**, 223–225.

Stewart, J. M., Kruger, G. J., Ammon, H. L., Dickinson, C. W. & Hall, S. R. (1972). The *XRAY72* system. Tech. Rep. TR-192. Computer Science Center, Univ. of Maryland, College Park, Maryland, USA.

Tuinstra, F. & Fraase Storm, G. M. (1978). *J. Appl. Cryst.* **11**, 257–259.

Wu, E. L., Lawton, S. L., Olson, D. H., Rohrman, A. C. Jr & Kokotailo, G. T. (1979). *J. Phys. Chem.* **83**, 2777–2781.